Wideband Subsurface Radar for Bridge Structural Health Monitoring and Nondestructive Evaluation

Tzuyang Yu[a], Che-Fu Su[a], Chieh-Ping Lai[b], and H. Felix Wu[c]

[a]Department of Civil and Environmental Engineering
University of Massachusetts Lowell, Lowell, MA 01854, U.S.A.
[b]LR Technologies, Inc.
Rockville, MD 20850, U.S.A.
[c]University of North Texas
Denton, TX 76203, U.S.A.

ABSTRACT

The nondestructive evaluation (NDE) inspection for building and bridge structures has attracted a lot of attentions for the fundamental research and the sensor system development. In this paper, development of a distant subsurface imaging radar is reported. Theoretical background of subsurface radar imaging is first provided. Experimental laboratory measurements using radar signals in the frequency range of 1-18 GHz were conducted. From the theoretical analysis and the initial experimental results on a laboratory reinforced concrete specimens, it is proved that the proposed subsurface imaging radar system can detect the location of steel reinforcement inside a concrete cylinder and identify the material property of panel specimens. Range-dependent attenuation of radar signals is experimentally studied using different materials. Findings are reported in the summary.

Keywords: : Bridge inspection, subsurface anomaly, radar NDE, synthetic aperture radar imaging, high gain antenna

1. INTRODUCTION

In the past two decades, radar and microwave sensors (e.g., ground penetrating radar, airborne radar, imaging radar, waveguide, coaxial probe) have been widely used in the nondestructive evaluation (NDE) and condition assessment of construction materials and transportation infrastructure systems. Reported applications include material characterization, anomaly detection, rebar detection, corrosion assessment, debonding/delamination detection, pavement thickness estimation, and remote sensing.[1] While radar and microwave sensors have gained success in the NDE of engineering materials/structures in other disciplines (e.g., military, aerospace), their direct applications in civil engineering are hampered by required inspection performance and complicated field conditions. For example, preliminary inspection of bridges must be conducted with high efficiency and at affordable cost in order to determine problematic areas for detailed inspection, while its resolution can be relatively-low. In view of the number of bridges to be inspected at a regulated frequency, specialized radar and microwave sensors must be developed to meet the practical needs from the field inspection of bridges.

In the design of radar and microwave sensors for the distant inspection of bridges, various issues must be addressed. For instance, the tradeoff between high range resolution and deep penetration depth is usually considered. A better down-range resolution suggests a wider frequency bandwidth, which can be achieved by an antenna designed for a higher frequency range. However, the path loss of radar and microwave signals also increases with the increase of frequency, resulting in lower penetration depth. Even the transmission power of the sensor can be amplified, the coupling between the transmitting antenna and reflections from the clutter may degrade the receiver sensitivity.

In this paper, development of a wideband subsurface imaging radar for the distant inspection of bridges is reported. Theoretical background of subsurface radar imaging (synthetic aperture radar or SAR) is first

Further author information: (Send correspondence to T. Yu)
E-mail: tzuyang_yu@UML.EDU, Telephone: 1 617 230 7402

Nondestructive Characterization for Composite Materials, Aerospace Engineering, Civil Infrastructure, and Homeland Security 2013, edited by Tzu Yang Yu, Andrew L. Gyekenyesi, Peter J. Shull, Aaron A. Diaz, H. Felix Wu,
Proc. of SPIE Vol. 8694, 86940I · © 2013 SPIE · CCC code: 0277-786X/13/$18 · doi: 10.1117/12.2010120

provided, followed by a series of laboratory experiments using radar signals in the frequency range of 1 GHz to 18 GHz. SAR images were generated by a two-dimensional laboratory positioning system at UMass Lowell. Material specimens of different sizes and compositions were used for SAR image calibration. Analysis of SAR images is also provided. Finally, research findings are discussed in the summary section.

2. DESIGN CONCEPT OF SUBSURFACE IMAGING RADAR

Critical transportation infrastructures like highway bridges can fail not only due to superstructure (girder, pier) failures, but also due to substructure (foundation) failures. Failures of bridges can be attributed to various causes including natural hazards (e.g., earthquake, storm, hurricane, flooding), service loads (e.g., dead load, traffic, snow, wind), man-made accidents (e.g., fire), and terrorism (e.g., explosion), in conjunction with material deterioration. Since bridges can fail due to various causes, and each cause can affect more than one bridge element to different extents, routine inspection must cover more than one bridge element. In a recent study based on the survey conducted by the National Bridge Inventory (NBI), the source of structural deficiency in highway bridges are more due to bridge superstructure and substructure than due to bridge deck.[2,3] Meanwhile, to achieve efficient inspection, spatial coverage of the sensor per inspection must be large enough to enable accelerated inspection, if necessary. Based on these considerations, a distant inspection scheme for bridges is illustrated in Figure 1. In Figure 1, reflected/returned radar measurements at different locations, frequencies,

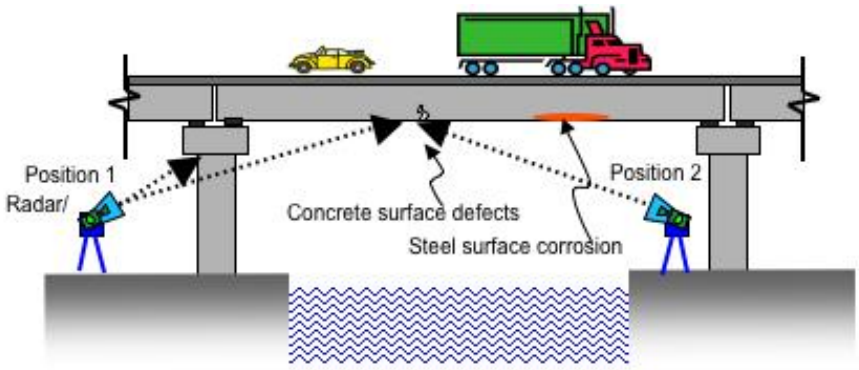

Figure 1. Proposed distant inspection scheme of a subsurface imaging radar system

relative elevations, inspection angles, and signal polarizations are collected and integrated by SAR imaging algorithms to render radar images for subsurface condition assessment. Depending on the information the radar sensor needs to learn from the returned signal, waveform types, frequency, and bandwidth can be designed to achieve the goal.

In the hardware design of the proposed subsurface imaging radar, high frequency signals in the frequency range of 1 GHz to 18 GHz are used. Wide bandwidth waveforms are chosen for their sensitivity to surface backscattering changes in radar signals. Monostatic and bistatic radar measurements are both explored in this development.

3. SUBSURFACE RADAR IMAGING

In the data processing of the wideband subsurface imaging radar system, reflected/returned radar signals are processed by synthetic aperture radar (SAR) and backprojection algorithms.[4,5] Primary steps in SAR imaging are described in the following. Define the coherent SAR point response collected by radar sensor as

$$S(x, y\sin\theta_i) = \text{sinc}\left(\frac{\pi y \sin\theta_i}{\rho_r}\right)\text{sinc}\left(\frac{\pi x}{\rho_{xr}}\right) \tag{1}$$

where (x, y, z) are coordinates on the plane of radar inspection, θ_i incident angle with respect to the z axis, ρ_r range resolution of the radar, and ρ_{xr} cross-range resolution of the radar. $\text{sinc(x)} = \dfrac{\sin(x)}{x}$ is the sinc function.

Define the distance between a single scatterer and the radar to be $\bar{r}_{s,j}$ where s denotes the scatterer and j the radar. Figure 2 illustrates the definition of inspection angle on the image plane. The coherent SAR point

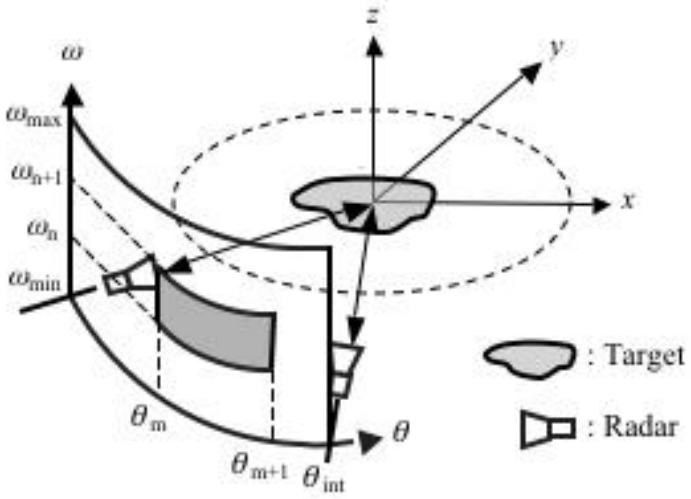

Figure 2. Definition of inspection angle on the image plane[5])

response can also be represented

$$S\left(\bar{r}_{s,j}\right) = \mathrm{sinc}\left(\frac{\pi r_{s,j}}{\rho}\right) \tag{2}$$

where $r_{s,j} = |\bar{r}_{s,j}|$ and $\rho = \sqrt{\rho_r^2 + \rho_{xr}^2}$. The time-dependent $S\left(\bar{r}_{s,j}\right)$ can be written by

$$S\left(\bar{r}_{s,j}, t\right) = \frac{1}{r_{s,j}^2} \int_{\omega_c - \pi B}^{\omega_c - \pi B} d\omega \cdot \exp\left[i\omega t\right] \tag{3}$$

where ω_c is the carrier frequency, B the frequency bandwidth, i the imaginary number, and t the time variable. The range compression on $S\left(\bar{r}_{s,j}, t\right)$ is conducted by shifting t to $\hat{t} = t - \dfrac{r_{s,j}}{c}$ (c is the speed of radar signals). The integral in Eq.(3) leads

$$S\left(\bar{r}_{s,j}, \hat{t}\right) = \frac{B}{r_{s,j}^2} \exp\left[i\omega_c \hat{t}\right] \cdot \mathrm{sinc}\left(B\hat{t}\right) \tag{4}$$

After performing range-compression on focused radar signals, we integrate all range-compressed focused radar signals to obtain $D\left(\xi, \hat{t}\right)$, where ξ is the position of the radar traveling on its synthetic aperture. The backprojection processing is conducted by

$$B_{BP}\left(\xi, t\right) = C_{BP} \cdot \frac{\partial D\left(\xi, \hat{t}\right)}{\partial t} \tag{5}$$

where C_{BP} is the backprojection coefficient defined in order to yield an ideal bandpass transfer function. Finally, the backprojected SAR image is obtained by

$$I\left(\bar{r}, \phi\right) = \int_0^{r_s \theta_{\mathrm{int}}} d\xi \cdot B_{BP}\left(\xi, \hat{t}\right) \tag{6}$$

where $(\bar{r}, \phi)$ is the polar coordinates on SAR images. It is noteworthy to point out that the resolution of SAR images can be further improved by bandwidth (B), frequency (ω_c), and synthetic aperture (θ_{int}). Time-space

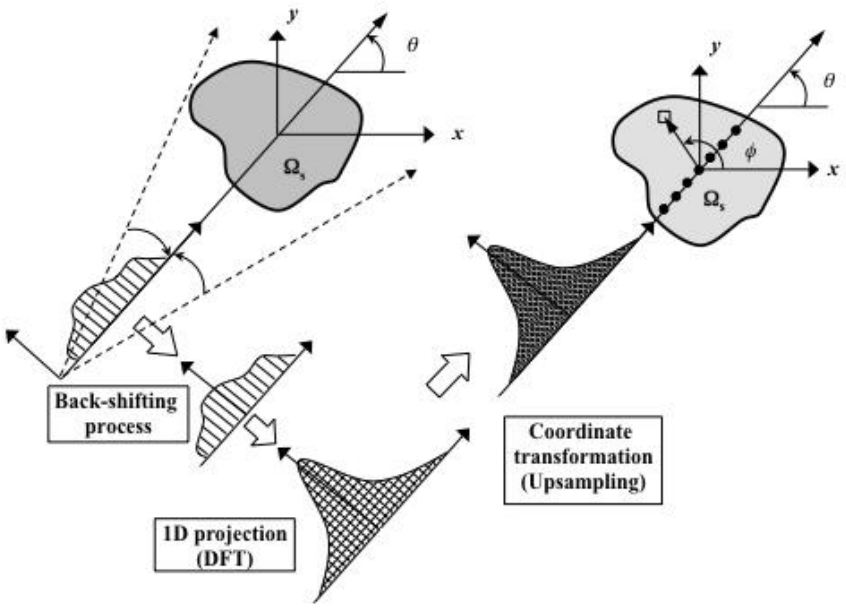

Figure 3. Concept of subsurface radar imaging (modified from[5])

projection is performed by the velocity of radar signals. SAR imaging and backprojection algorithms have been demonstrated as a promising technique in the subsurface sensing of construction materials. Their use on the detection of subsurface debonding in multi-layer composite-concrete systems has also been reported.[6] Additional information on the remote sensing theories can be found in the literature.[7–9]

4. LABORATORY RADAR MEASUREMENTS

To validate the performance of proposed subsurface imaging radar, an anechoic chamber was designed and constructed for collecting laboratory distant radar responses of specimens. Figure 4 shows the anechoic chamber custom-built for the distant radar measurement in the frequency range of 1 GHz to 18 GHz. With the current configuration, the maximum distance is approximately 3 m or 10 ft. The distance between the radar and the specimen is adjustable, and the radar scanning is controlled by a two-dimensional positioning system. The radar system can perform linear scan or circular scan in the laboratory at UML. Various specimens were measured

Figure 4. Custom-built anechoic chamber, 1 GHz-18 GHz; (left) exterior of the chamber, (right) interior of the chamber with a reinforced concrete beam specimen (CEE, UML)

by the radar system for calibrating signal attenuation on different materials, including a 1ft-by-1ft-1in plain concrete slab, a 2ft-by-1ft-by-0.5in steel plate, and a X-by-Y-by-Z brass plate. A typical SAR image generated by linear scan is provided in Figure , using the plain concrete slab as an example. In Figure 3, actual location

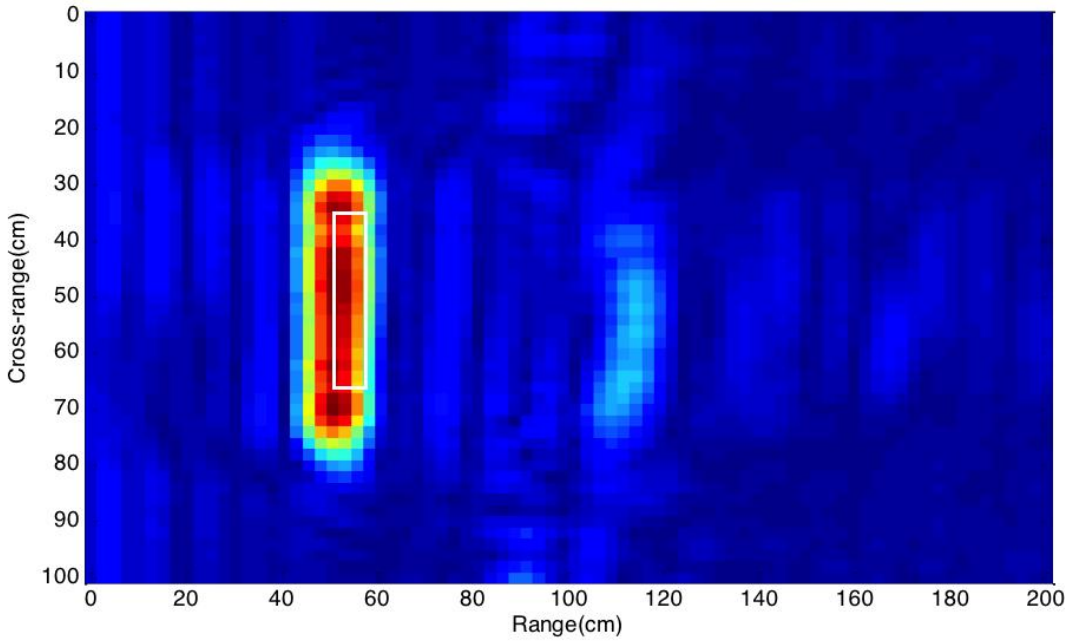

Figure 5. Linear scan SAR image of a plain concrete slab, range = 50 cm

of the concrete slab is indicated. Specular returns from the surface of the slab, as well as the edge diffraction effects, are clearly observed in Figure 3. Fluctuation of SAR amplitude indicates the surface roughness and material homogeneity of the specimen. Using the maximum SAR response $I_{\max}$, three specimens were measured at different distances/ranges. In Figure 6, attenuation of maximum SAR amplitudes is found. Specimens made of different materials and sizes show different attenuation patterns. This nonlinear drop of maximum SAR amplitude, as a function of range, exhibits an reducing slope with the increase of range. Since the attenuation pattern of SAR amplitudes depends on the size, shape, and material property of the specimen, a database will be developed for predicting the background response of different structures.

Concrete cylinders with and without an embedded No. 4 steel rebar were measured by the radar system for subsurface rebar detection. Figures 7 and 8 show the concrete cylinders and their SAR images. After subtracting the background response (plain concrete) from the total response (reinforced concrete), the differential SAR image is shown in Figure 9. In Figure 9, a strong scatter in the subtracted SAR image is found at the actual location where the rebar is located, demonstrating the subsurface sensing capability of the radar system. Meanwhile, importance of the background signal is realized.

5. SUMMARY

Efficient and effective bridge inspection must accommodate the needs from accessibility and damage detectability. Other than surface sensing techniques, subsurface sensing represents a technological capability that enables early-warning in the routine maintenance of bridges. SAR imaging and backprojection algorithms have been shown as a promising technique in the subsurface sensing of construction materials using electromagnetic waves (radar signals). Reflected radar signals collected at a distance can be used to reconstruct the subsurface radar images of structures. Resolution of SAR images can be further improved by bandwidth, frequency, and synthetic aperture. On the other hand, portability of a field subsurface imaging radar system can be affected by the design specs

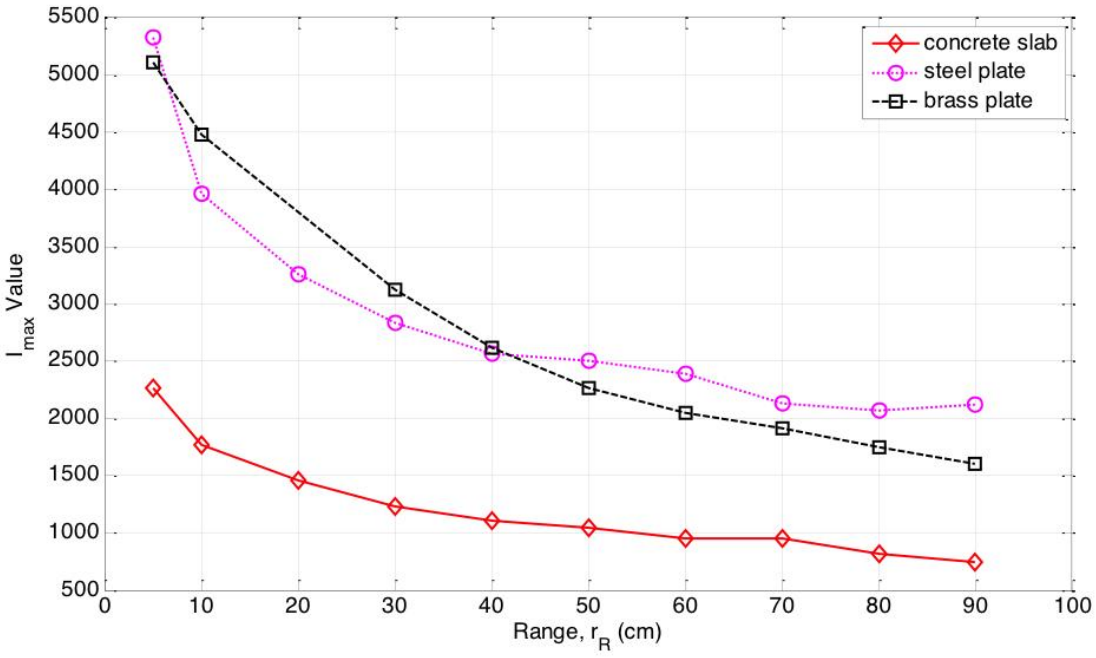

Figure 6. Maximum SAR amplitude of three specimens at different ranges

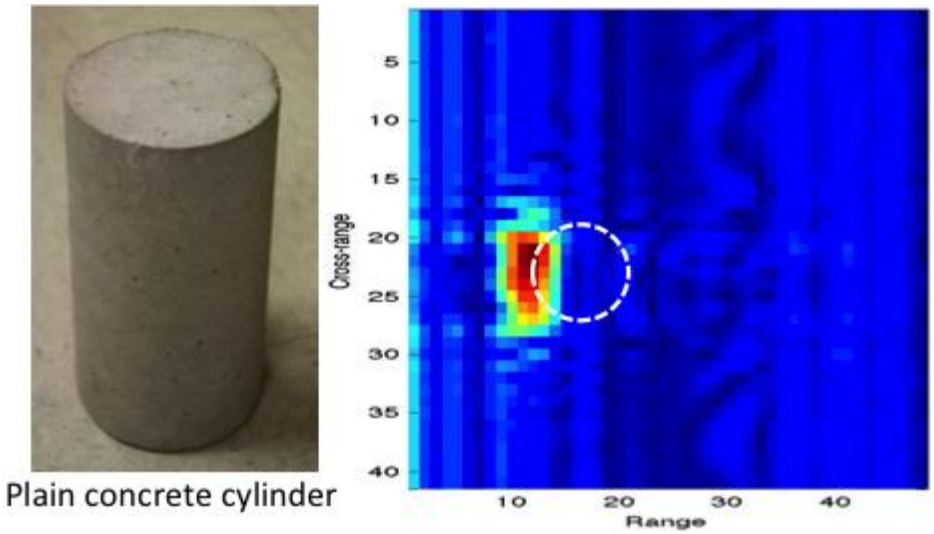

Figure 7. Plain concrete cylinder and its SAR image

such as synthetic aperture and minimum frequency. A robust field radar system can only be developed with a series of comprehensive laboratory tests to thoroughly understand the background signal encountered in the field.

6. ACKNOWLEDGMENTS

This work was supported by the U.S. Department of Transportation (DOT) Research and Innovative Technology Administration (RITA) Commercial Remote Sensing and Technology (CRS&SI) Program. Laboratory experimental work was assisted by Shafique Ahmed and Ross Gladstone from UML.

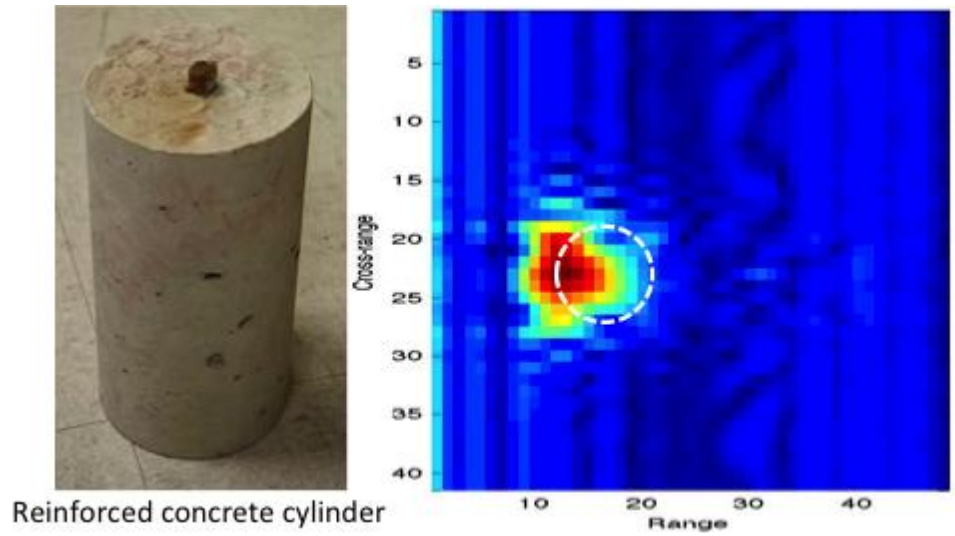

Figure 8. Plain concrete cylinder with an embedded steel rebar and its SAR image

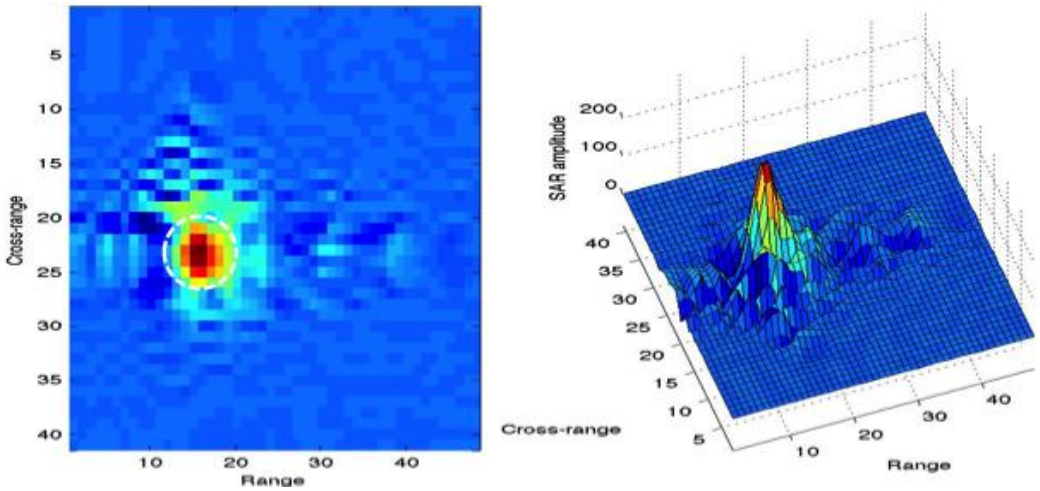

Figure 9. Subtracted SAR image

7. DISCLAIMER

The views, opinions, findings and conclusions reflected in this presentation are the responsibility of the authors only and do not represent the official policy or position of the USDOT/RITA, or any State or other entity.

REFERENCES

[1] Yu, T.-Y. and Buyukozturk, O., "A far-field radar ndt technique for detecting debonding in gfrp-retrofitted concrete structures," *NDT&E Intl.* **4**, 10–24 (2008).

[2] (FHWA), F. H. A., "Highway bridge inspection: State-of-the-practice survey," **FHWA-RD-01-033**, NDE Validation Center, McLean, VI (2001).

[3] (NBI), N. B. I., [*2006 Status of the Nation?s Highways, Bridges, and Transit: Conditions and Performance*], Federal Highway Administration, Washington, D.C. (2007).

[4] Yegulalp, A. F., "Fast backprojection algorithm for synthetic aperture radar," in [*Proc. of IEEE Radar Conf.*], 60–5, IEEE (1999).

[5] Yu, T., "A distant damage assessment method for multi-layer composite systems using electromagnetic waves," *J. Eng. Mech.* **137**(8), 547–560 (2011).

[6] Yu, T.-Y., "Determining the optimal parameters in a distant radar nde technique for debonding detection of gfrp-concrete systems," in [*Proc. SPIE*], **7294** (2009).
[7] Soumekh, M., [*Synthetic aperture radar signal processing with MATLAB algorithms*], Wiley, New York, NY (1999).
[8] Kong, J. A., [*Electromagnetic Wave Theory*], EMW Publishing, Cambridge, MA (2000).
[9] Tsang, L., Kong, J. A., and Ding, K.-H., [*Scattering of Electromagnetic Waves – Theories and Applications*], John Wiley & Sons, New York (2000).